A SIMULATION STUDY OF THE ROTOR VIBRATION IN A JOURNAL BEARING

Jiří Tůma*, Alena Bilošová**, Jiří Šimek***, Rudolf Svoboda***

The paper deals with the rotor vibration in journal bearings to prepare a model for verifying the rotor vibration active control. The rotor is maintained in equilibrium position by forces generated in oil film. Bearing forces can be modelled as a spring and damper system. The main goal of the simulation study is to verify the model principle and to estimate parameters by comparing simulation results with experimental data, namely the instability of motion. Test stand with rotor supported in two journal bearings was designed for these purposes. The stand will be equipped with four piezoactuators enabling excitation of bearings by practically arbitrary dynamic force. Theoretical analysis of the influence of external excitation on rotor behaviour was carried out. Up to now the study shows, that simple kinematic excitation is effective for reducing rotor excursion while passing critical speeds. To suppress self-exciting vibration of the rotor it is necessary to look for more sophisticated solution.

Key words: *rotor stability, hydrodynamic journal bearing, vibration active control, piezoactuators, proximity probes*

1. Introduction

There are many ways how to model a rotor system, but this paper prefers an approach, which is based on

- the concept developed by Muszynska [1, 7] and supported by Bently Rotor Dynamics Research Corporation.
- the lubricant flow prediction using a FE method for Reynolds equation solution.

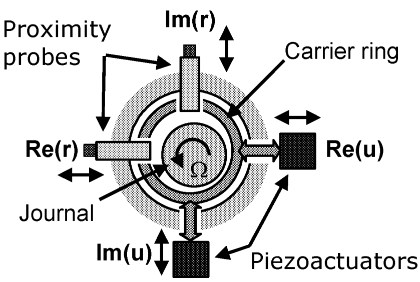

Fig.1: Journal coordinates

The reason for using Muszynska approach is that this concept offers an effective way to understand the rotor instability problem and to model a journal vibration active control system by manipulating the sleeve position by actuators [2], which are a part of the closed loop composed of proximity probes and a controller. The solution based on Reynolds equation gives more precise dynamic characteristics of the rotor including rotor stability threshold, see [3] for instance.

* prof. Ing, J. Tůma, CSc., Department of Control Systems and Instrumentation, Faculty of Mechanical Engineering, VSB – Technical University of Ostrava, 17. listopadu 15, CZ-708 33 Ostrava, Czech Republic
** Ing. A. Bilošová, Ph.D., Department of Mechanics, Faculty of Mechanical Engineering, VSB – Technical University of Ostrava, 17. listopadu 15, CZ-708 33 Ostrava, Czech Republic
*** Ing. J. Šimek, Mgr. R. Svoboda, CSc., TECHLAB s.r.o., Sokolovská 207, 190 00 Praha 9, Czech Republic

The arrangement of proximity probes and piezoactuators in a rotor system is shown in figure 1. Let the rotor angular velocity is designated by Ω. It is assumed that the sleeve as a carrier ring of the journal bearing is a movable part in two perpendicular directions while rotor is rotating. This paper proposes to use complex variables to describe motion of the rotor and the carrier ring in the complex plane. The position of the journal centre in the complex plane, origin of which is situated in the bearing centre, is designated by a position vector $\mathbf{r}$. The position of the carrier ring is determined by a position vector $\mathbf{u}$.

2. Muszynska lumped parameter model of the rotor system

The internal spring, damping and tangential forces are acting on the rotor. As Muszynska has stated these bearing forces can be modeled as a rotating spring and damper system at the angular velocity $\lambda\,\Omega$ (see figure 2), where λ is a parameter, which is slightly less than 0.5. The parameter λ is denominated by Muszynska [1] as the fluid averaged circumferential velocity ratio. The external forces refer to forces that are applied to the rotor, such as preloads in the form of constant radial forces. The fluid pressure wedge is the actual source of the fluid film stiffness in a journal bearing and maintains the rotor in equilibrium. To simplify modeling in Matlab-Simulink, the quantities in this chapter, like force, velocity and displacement, are position vectors which coordinates are determined by complex numbers. Fluid forces acting on the rotor in coordinates rotating at the same angular frequency as the spring and damper system are given by the formula

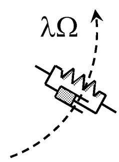

Fig.2: Model of oil film

$$\mathbf{F}_{\mathrm{rot}} = K\,(\mathbf{r}_{\mathrm{rot}} - \mathbf{u}_{\mathrm{rot}}) + D\,(\dot{\mathbf{r}}_{\mathrm{rot}} - \dot{\mathbf{u}}_{\mathrm{rot}})\ , \tag{1}$$

where the parameters, K and D, specify proportionality of stiffness and damping to the relative position of the journal centre displacement vector $\mathbf{r}_{\mathrm{rot}} - \mathbf{u}_{\mathrm{rot}}$ and velocity vector $\dot{\mathbf{r}}_{\mathrm{rot}} - \dot{\mathbf{u}}_{\mathrm{rot}}$, respectively. The equation of motion without an active control $\mathbf{u} = \mathbf{0}$ is as follows

$$M\,\ddot{\mathbf{r}} + D\,\dot{\mathbf{r}} + (K - \mathrm{j}\,D\,\lambda\,\Omega)\,\mathbf{r} = m\,r_{\mathrm{u}}\,\omega^2\,\exp[\mathrm{j}\,(\omega\,t + \delta)]\ , \tag{2}$$

where M is the total rotor mass. The unbalance force, which is produced by unbalance mass m mounted at a radius r_{u}, acts in the radial direction and has a phase δ at time $t = 0$ [4].

The frequency transfer function relating a harmonic force $\mathbf{F}$ at the angular frequency ω to the centerline position $\mathbf{r}$ is given by the following formula

$$G_{\mathrm{Fr}}(\mathrm{j}\,\omega) = \frac{\mathbf{r}(\mathrm{j}\,\omega)}{\mathbf{F}(\mathrm{j}\,\omega)} = \frac{1}{K - M\,\omega^2 + \mathrm{j}\,(\omega\,D - \lambda\,\Omega\,D)}\ . \tag{3}$$

3. Simulink model of the rotor system

The equation of motion (2) contains a complex vector $\mathbf{r}(t)$, as an unknown function of time, and the equation parameters are complex quantities as well. The complex function can be replaced by the real and imaginary functions and solved as many similar models. In this paper, the connecting blocks by complex signals are preferred. The Simulink block diagram for the motion equation is shown in figure 3. The system is excited by an unbalance force rotating at the same angular velocity Ω (OMEGA) as the rotor and by the non-synchronous perturbation force rotating by the angular velocity ω (omega), amplitude of which is proportional to the square of the angular velocity.

The parameters K and D, specifying oil film stiffness and damping, are a function of the position vector. The values of these parameters are determined by the oil film thickness. It is assumed that it is possible to approximate both these functions by formulas

$$K = \frac{K_0}{1 - \left(\frac{|\mathbf{r}|}{e}\right)^n} \ , \qquad D = \frac{D_0}{1 - \left(\frac{|\mathbf{r}|}{e}\right)^n} \ , \tag{4}$$

where e is a journal bearing clearance and n is a power. The form of the functions (4) assumes that the influence of the oil film thickness on the value of the mentioned parameter is the same. It is required that the functions (4) has to be continuously differentiable (a smooth function) at $\mathbf{r} = \mathbf{0}$. It means that the first derivative with respect to time at $\mathbf{r} = \mathbf{0}$ has to be equal to zero, which implies that the power n has to be greater than unity ($n > 1$). The best agreement between simulation and measurement results was reached for the value of the exponent, which is equal to 1.1 .

As the rotor system stability margin depends on the oil film stiffness and rotor mass, the first step is to estimate the parameter K. This task is not an easy problem due to the rotor static load by the gravity force and the dependence of the oil film stiffness on the rotor eccentricity. The second problem is an estimation of the parameter D, which predefines the rotor system vibration mode at the angular frequency, which is approximately equal to the half of the rotor angular frequency.

The agreement between the mentioned experiment and the simulation model is reached for the following values of the parameters:

$M = 1.6\,\mathrm{kg}$ .... rotor mass
$lam = 0.475$ .... fluid averaged circumferential velocity ratio (lambda)
$K_0 = 4000\,\mathrm{N/m}$ .... oil film stiffness
$D_0 = 1000\,\mathrm{Ns/m}$ .... oil film damping coefficient
$n = 1.1$ .... exponent in the formula (4)
$e = 0.0002\,\mathrm{m}$ .... clearance in the journal bearing
$m\,r_\mathrm{u} = 0.00001\,\mathrm{kgm}$ ..... product of the unbalance mass m mounted at a radius r_u.

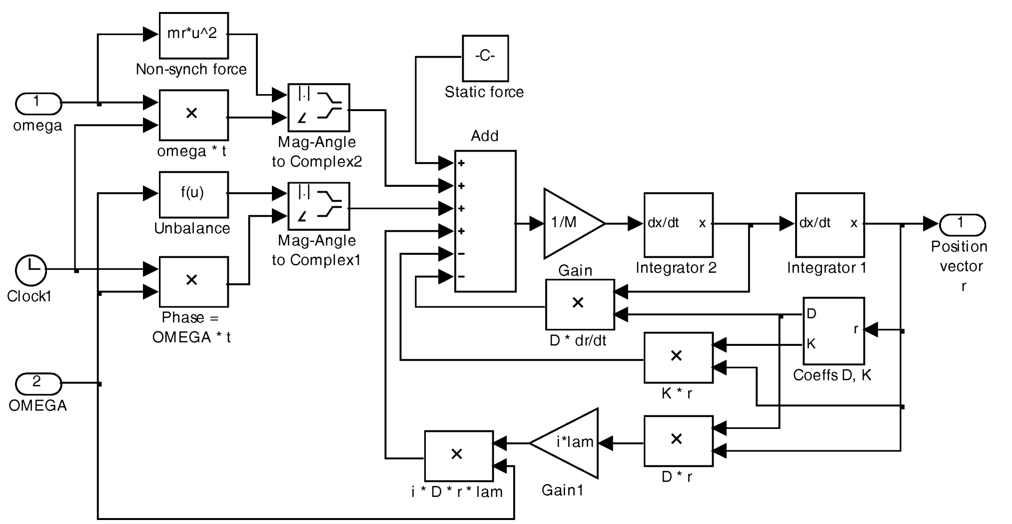

Fig.3: Model of a journal motion in a plane perpendicular to the rotor axis

The value of the product $m\,r_{\mathrm{u}}$ corresponds to the ISO balance quality grade between G 1 and G 2.5 at 2500 rpm. Note the variation in the journal position during the rotor run up in the right up diagram in figure 4. The experiments show that if the rotor is in an unstable state (vibration are limited only by the bearing wall), then the frequency of vibration is slightly less than half the rotor rotational frequency Ω. The ZOOMs of the position vector real and imaginary parts just before and after the vibration onset, which are shortened into the time interval of 0.2 s, are shown in the bottom diagrams in figure 4. Comparison of the number of waves in the time intervals of the same length shows that the frequency of vibration drops to half the frequency before the vibration onset. The orbit plots for simulation and measurements on the Bently Nevada Rotorkit RK 4 are shown in figure 5. It should be mentioned that the measurements were performed at room temperature about 20 °C, oil pressure 1.5 psi (10.3 kPa). It can be concluded that the behaviour of the simulation model and the true rotor system is the same. All the simulations are done by using Matlab-Simuling with the variable integration step and the ODE45 integration method.

As the measurement of the rotor system response to the non-synchronous perturbation is not available yet, the simulation is replaced by the evaluation of the frequency response magnitude (3) as a function of the dimensionless frequency f/f_{rot}, which is shown in figure 6. The magnitudes of the frequency response on the figure left side are evaluated for the rotor steady-state speed 1800 rpm and for some multiples (1×, 2×, 5× and 10×) of the initial values of the parameters K and D. The resonant frequency is approximately at the mentioned dimensionless frequency λ, i.e. slightly less then 0.5 . The magnitudes of the frequency response on the figure right side differ in the value of the parameter D. As the experiments [5] show that the resonant frequency is greater than the dimensionless frequency 0.4, the assumed relationship between the values of K and D seems to be good. The experimental results agree with simulation.

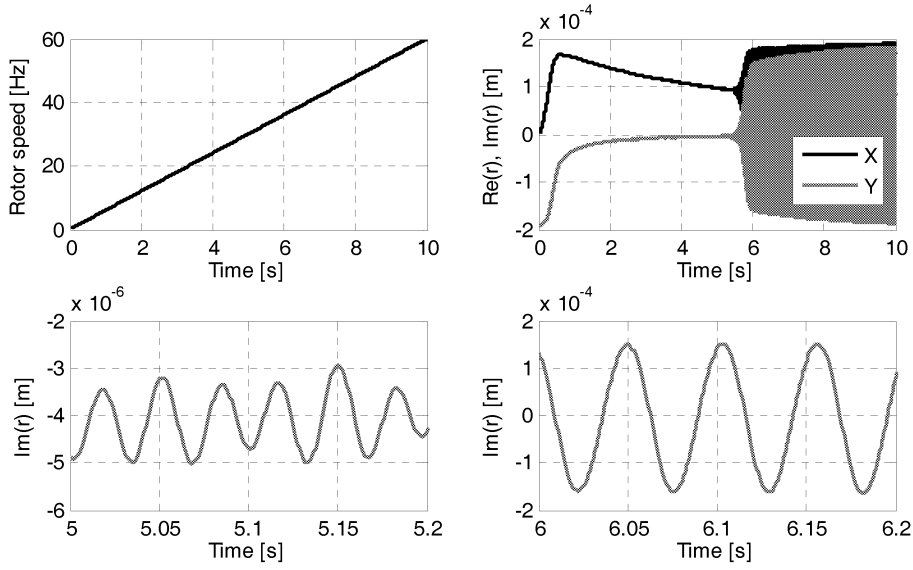

Fig.4: Time history of the rotational frequency and journal centreline coordinates up to the moment when fluid induced vibration starts up and ZOOM of the journal centreline coordinate time history just before and after the vibration onset

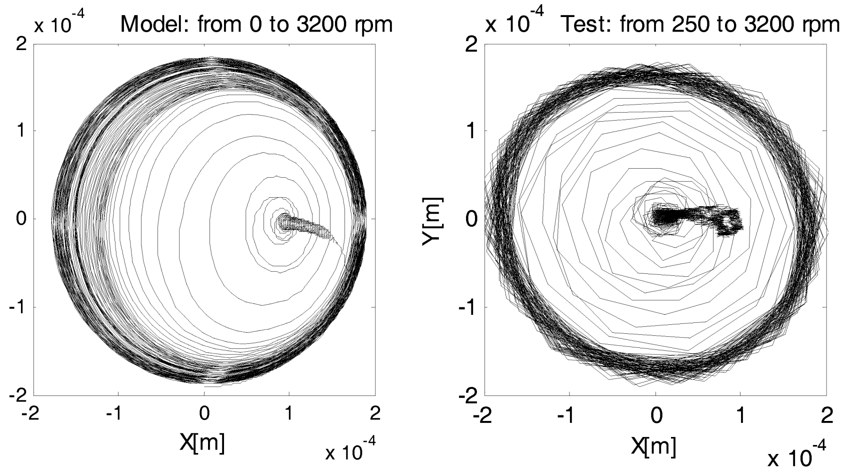

Fig.5: Comparison of the orbit simulation and measurement

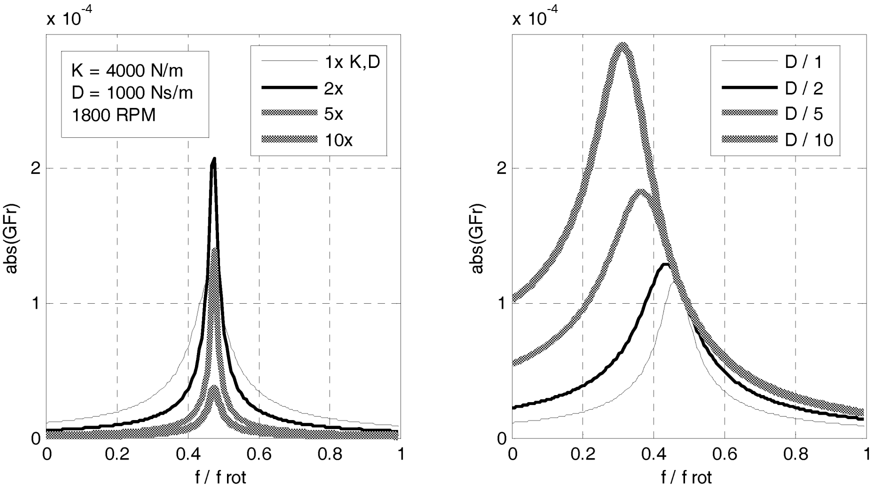

Fig.6: The frequency response magnitude as a function of the dimensionless perturbation force rotational frequency related to the rotor rotational frequency

4. Experimental stand

For investigation of the rotor active control it is necessary to run the rotor up its stability limit. Test stand (figure 7) was designed with bearing diameter of 30 mm, which enabled to design the rotor both rigid and light, thus achieving low stability limit.

The base of the stand is the frame 1 composed of hollow aluminium profiles. High frequency motor 3, fixed in clamping plate 2, is connected to the test shaft 7 by elastic coupling 6. The motor, enabling to reach speeds over 20 000 rpm, is supplied by high-frequency current from converter with possibility of control by PC. The elastic coupling of the multi-plate type constitutes two joints, thus separating the shaft from the drive. Bearing pedestals 5 contain bearing bushings, inserted into pedestals with clearance. The bearing bushings are connected by means of screw bars to two vertically and two horizontally arranged piezoactuators 12. Piezoactuators are secured in frames 13 and 14 respectively,

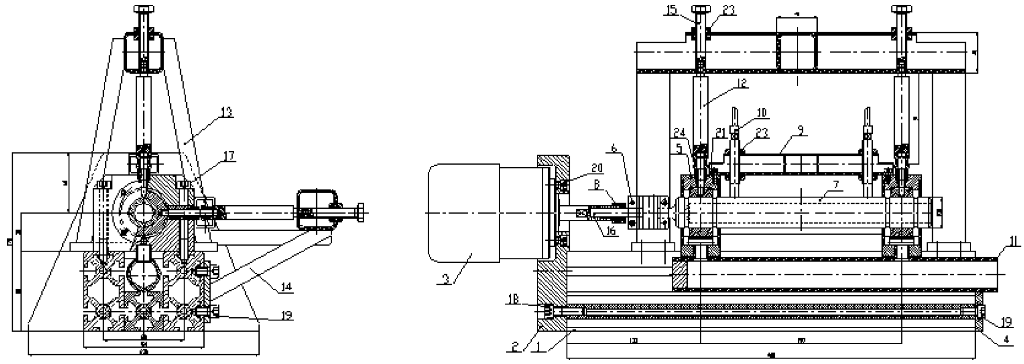

Fig.7: Test stand for experimental investigation of the rotor active control

which are fastened to the stand base. Piezoactuators have maximum deviation of 60 μm, maximum force in tension/pressure 800/300 N. Four relative vibration sensors 10, fixed in carriers 9 fastened to bearing pedestals, enable tracing of the shaft movement in both bearings. The bearings of circular cross section were designed with clearance resulting in calculated stability limit of about 11 000 rpm. The rigid shaft can be eventually replaced by an elastic one, enabling tests of running through bending critical speeds of the rotor.

5. Theoretical analysis – kinematic excitation of bearings

In contrast to the previous chapter, model analysis will deal with quantities arranged into vectors and matrices. Contrary to the scalar variables, vectors and matrices are always designated by bold characters, matrices in addition by capitals. As the shaft centreline position was designated previously by $\mathbf{r}$ in the meaning of the distance from the bearing centreline, it was changed to $\mathbf{x}$ or $\mathbf{y}$ to emphasise its real coordinate structure in rotor models with multiple degrees of freedom. In general, all vector and matrix variables relative planar motion of a mass point will be of order 2, whereas order of variables relative rotor model will be determined by actual model dimensions.

As follows from the Reynold's equation of hydrodynamic lubrication [6], hydrodynamic bearing forces acting on the shaft represent in general a non-linear vector function of the shaft position $\mathbf{x}_\mathrm{b}$ in the bearing and a linear function of its velocity $\dot{\mathbf{x}}_\mathrm{b}$:

$$\mathbf{f}_\mathrm{H}(\mathbf{x}_\mathrm{b}, \dot{\mathbf{x}}_\mathrm{b}, \omega) \equiv \mathbf{k}_\mathrm{H}(\mathbf{x}_\mathrm{b}, \omega) + B_\mathrm{H}(\mathbf{x}_\mathrm{b}, \omega)\, \dot{\mathbf{x}}_\mathrm{b} \ . \tag{5}$$

In case of zero velocity, when shaft is rotating around its longitudinal axis, for each angular velocity ω there exists corresponding static equilibrium position $\mathbf{x}_0(\omega)$, in which the bearing load vector $\mathbf{q}_\mathrm{b}$ is balanced by hydrodynamic force. Supposing small vibrations around this equilibrium position, hydrodynamic bearing force can be linearized, i.e. replaced by first two terms of Taylor series

$$\mathbf{f}_\mathrm{H}(\mathbf{x}_\mathrm{b}, \dot{\mathbf{x}}_\mathrm{b}, \omega) \approx \mathbf{k}_\mathrm{H}(\mathbf{x}_\mathrm{b0}, \omega) + \frac{\partial \mathbf{k}_\mathrm{H}}{\partial \mathbf{x}}\, (\mathbf{x}_\mathrm{b} - \mathbf{x}_\mathrm{b0}) + B_\mathrm{H}(\mathbf{x}_\mathrm{b0}, \omega)\, \dot{\mathbf{x}}_\mathrm{b} \ . \tag{6}$$

Introducing a relative shaft journal displacement with respect to this equilibrium position $\mathbf{y}_\mathrm{b} = \mathbf{x}_\mathrm{b} - \mathbf{x}_\mathrm{b0}$ and relative velocity $\dot{\mathbf{y}}_\mathrm{b} = \dot{\mathbf{x}}_\mathrm{b} - \dot{\mathbf{x}}_\mathrm{b0} \equiv \dot{\mathbf{x}}_\mathrm{b}$, hydrodynamic bearing force can be approximated by relation

$$\mathbf{f}_\mathrm{H}(\mathbf{x}_\mathrm{b}, \dot{\mathbf{x}}_\mathrm{b}, \omega) \approx -\mathbf{q}_\mathrm{b} - \mathbf{K}_\mathrm{b}(\omega)\, \mathbf{y}_\mathrm{b} - \mathbf{B}_\mathrm{b}(\omega)\, \dot{\mathbf{y}}_\mathrm{b} \ , \tag{7}$$

where $K_\mathrm{b}(\omega) = -\frac{\partial \mathbf{k}_\mathrm{H}}{\partial \mathbf{x}}(\mathbf{x}_{\mathrm{b}0}(\omega),\omega)$ and $\mathbf{B}_\mathrm{b}(\omega) = -\mathbf{B}_\mathrm{H}(\mathbf{x}_{\mathrm{b}0}(\omega),\omega)$ are so called stiffness and damping matrices of the oil film in equilibrium position $\mathbf{x}_{\mathrm{b}0}(\omega)$.

General non-linear description of bearing forces is necessary to study rotor systems with big excursions of the shaft in the bearings. Unlike the linearized case, where sophisticated methods of finding stiffness and damping bearing matrices are known, to find the full non-linear description of the field of hydrodynamic forces in the whole bearing clearance range remains still a problem. Non- linear forces have to be determined numerically on the sufficiently fine net, which requires huge amount of calculations and data. An analytical formulation of non-linear bearing forces can be derived only for special simplified cases of so-called 'short' or 'long' circular bearings.

With respect to intended purposes of decreasing and shifting resonance peaks in critical speeds as well as for improvement of rotor stability (both mentioned phenomena occur in the linear range of small shaft displacements in the bearing), linear description of hydrodynamic bearing forces is fully adequate. Dynamic properties of the bearings are then described by a sequence of stiffness and damping matrices defined in a succession of equilibrium positions, which correspond to the succession of shaft speeds $\{\omega_j\}$ covering whole operating speed range.

The rotor shaft itself represents a linear dynamic system, which can be modelled by means of standard finite element discretization procedures, leading to description of the system by mass, stiffness and gyroscopic matrices $\mathbf{M}_\mathrm{s}$, $\mathbf{K}_\mathrm{s}$, $\mathbf{D}_\mathrm{s}$ and displacement vector $\mathbf{x}$; its sub-vectors $\mathbf{x}_k$ (of length 4) represent deflection and tilting in connections of two adjacent finite elements. The complete rotor and oil film and bearing bushing system can be described by two equations, the first one for shaft motion, the second one for bushings:

$$\begin{aligned} \mathbf{M}_\mathrm{s}\,\ddot{\mathbf{x}} + \omega\,\mathbf{G}_\mathrm{s}\,\dot{\mathbf{x}} + \mathbf{K}_\mathrm{s}\,\mathbf{x} &= \mathbf{n}(\omega,t) + \mathbf{g} + \mathbf{f}_\mathrm{H}(\mathbf{x}_\mathrm{L}-\mathbf{x}_\mathrm{p},\dot{\mathbf{x}}_\mathrm{L}-\dot{\mathbf{x}}_\mathrm{p},\omega)\ , \\ \mathbf{M}_\mathrm{p}\,\ddot{\mathbf{x}}_\mathrm{p} + \mathbf{B}_\mathrm{p}\,\dot{\mathbf{x}}_\mathrm{p} + \mathbf{K}_\mathrm{p}\,\mathbf{x}_\mathrm{p} &= \mathbf{g}_\mathrm{p} - \mathbf{f}_\mathrm{H}(\mathbf{x}_\mathrm{L}-\mathbf{x}_\mathrm{p},\dot{\mathbf{x}}_\mathrm{L}-\dot{\mathbf{x}}_\mathrm{p},\omega) + \mathbf{f}_\mathrm{A}(t,\boldsymbol{\alpha},\mathbf{x}(t),\mathbf{x}_\mathrm{p}(t),\dots)\ . \end{aligned} \tag{8}$$

In these equations vector $\mathbf{x}_\mathrm{p}$ denotes deflections of bushings, $\mathbf{B}_\mathrm{p}$ and $\mathbf{K}_\mathrm{p}$ damping and stiffness matrices of bushing seat, $\mathbf{g}$, $\mathbf{g}_\mathrm{p}$ weight vectors of shaft and bushings, $\mathbf{n}(\omega,t)$ vector of external unbalance forces, $\mathbf{f}_\mathrm{H}$ hydrodynamic forces acting on the shaft at bearing locations, $\mathbf{f}_\mathrm{A}$ exciting forces acting on the bushings.

In case of linearized description of hydrodynamic bearing forces (on condition of small shaft excursions in the bearing), the static part of these forces is in balance with load vectors and dynamic part is described by means of stiffness and damping matrices. Introducing a relative shaft displacement vector $\mathbf{y}$, where displacements are taken relatively to the joint line of (static) equilibrium position in both bearings, the above equations transform to the system

$$\begin{aligned} \mathbf{M}_\mathrm{s}\,\ddot{\mathbf{y}} + [\omega\,\mathbf{G}_\mathrm{s} + \tilde{\mathbf{B}}_\mathrm{b}(\omega)]\,\dot{\mathbf{y}} + [\mathbf{K}_\mathrm{s} + \tilde{\mathbf{K}}_\mathrm{b}(\omega)]\,\mathbf{y} &= \mathbf{n}(\omega,t) - (\mathbf{M}_\mathrm{s}\,\mathbf{P}\,\ddot{\mathbf{x}}_\mathrm{p} + \omega\,\mathbf{G}_\mathrm{s}\,\mathbf{P}\,\dot{\mathbf{x}}_\mathrm{p})\ , \\ \mathbf{M}_\mathrm{p}\,\ddot{\mathbf{x}}_\mathrm{p} + \mathbf{B}_\mathrm{p}\,\dot{\mathbf{x}}_\mathrm{p} + \mathbf{K}_\mathrm{p}\,\mathbf{x}_\mathrm{p} &= \mathbf{f}_\mathrm{a}(t,\boldsymbol{\alpha},\mathbf{x}(t),\mathbf{x}_\mathrm{p}(t),\dots) + \mathbf{B}_\mathrm{b}(\omega)\,\dot{\mathbf{y}}_\mathrm{b} + \mathbf{K}_\mathrm{b}(\omega)\,\mathbf{y}_\mathrm{b}\ . \end{aligned} \tag{9}$$

$\tilde{\mathbf{B}}_\mathrm{b}(\omega)$, $\tilde{\mathbf{K}}_\mathrm{b}(\omega)$ denote the shaft-system related matrices with bearing matrices $\mathbf{B}_\mathrm{b}(\omega)$, $\mathbf{K}_\mathrm{b}(\omega)$ at appropriate positions and transformation matrix $\mathbf{P}$ ensures a linear distribution of bushing displacements along the shaft.

Excitation forces acting on bearing bushings, which are generated by piezoactuators, are formally represented by force vector $\mathbf{f}_\mathrm{a}$ in dependence on parameters $\boldsymbol{\alpha}$ and shaft and bearing displacements $\mathbf{y}$ and $\mathbf{x}_\mathrm{p}$ respectively. The resulting effect of this additional bearing excitation on rotor dynamics will strongly depend on their form and functional relations. Based on the kind and character of generated excitation such rotor systems can be divided into three basic groups:

I. Rotors with kinematic excitation of bearing bushings,
II. Rotors with parametric excitation of bearing bushings,
III. Rotors with active control of exciting forces.

In case of kinematic excitation the exciting force acting on the bushings is independent on shaft or bushing deflections and represents therefore another external excitation, which can have (contrary to unbalance) arbitrary non-synchronous frequency. If the source of exciting force is sufficiently robust, kinematic trajectory instead of kinematic force can be prescribed. As will be shown, kinematic excitation enables to change the course of response, but does not influence rotor stability.

In both remaining cases the exciting forces acting on bushings are generated in such a way, that either in dependence on the bearing deflections simulate periodically variable stiffness of bearing bushings (parametric excitation) or in appropriate manner respond to the deflection at specified shaft location (active control). Through parametric excitation as well as active control both rotor stability and rotor response can be affected. These problems are now deeply studied and results will be published later.

Provided that kinematic trajectories of bearing bushings are prescribed, the rotor system is defined by a single linear differential equation

$$\mathbf{M}_\mathrm{s}\,\ddot{\mathbf{y}} + [\omega\,\mathbf{G}_\mathrm{s} + \tilde{\mathbf{B}}_\mathrm{b}(\omega)]\,\dot{\mathbf{y}} + [\mathbf{K}_\mathrm{s} + \tilde{\mathbf{K}}_\mathrm{b}(\omega)]\,\mathbf{y} = \mathbf{n}(\omega,t) - (\mathbf{M}_\mathrm{s}\,\mathbf{P}\,\ddot{\mathbf{x}}_\mathrm{p} + \omega\,\mathbf{G}_\mathrm{s}\,\mathbf{P}\,\dot{\mathbf{x}}_\mathrm{p})\ . \qquad (10)$$

As the bearing deflections $\mathbf{x}_\mathrm{p}$ are known, the second term on the right side of equation represents (analogously to unbalance force) another excitation force only. As a linear system this equation can be solved by standard methods. The frequency and modal properties of the system are determined by corresponding eigenvalue problem

$$\mathbf{S}(\lambda,\omega)\,\hat{\mathbf{y}} = \left\{\lambda^2\,\mathbf{M}_\mathrm{s} + \lambda\,[\omega\,\mathbf{G}_\mathrm{s} + \tilde{\mathbf{B}}_\mathrm{b}(\omega)] + [\mathbf{K}_\mathrm{s} + \tilde{\mathbf{K}}_\mathrm{b}(\omega)]\right\}\hat{\mathbf{y}} = \mathbf{0}\ , \qquad (11)$$

while time-response amplitudes are given by relation

$$\mathbf{y}(t) = \mathrm{Re}\left\{\mathbf{S}^{-1}(\mathrm{i}\,\omega,\omega)\,\vec{\mathbf{n}}\,\omega^2\,\mathrm{e}^{\mathrm{i}\,\omega\,t}\right\} - \mathrm{Re}\left\{\mathbf{S}^{-1}(\mathrm{i}\,\Omega,\omega)\,(-\Omega^2\,\mathbf{M}_\mathrm{s}\,\mathbf{P} + \mathrm{i}\,\Omega\,\omega\,\mathbf{G}_\mathrm{s}\,\mathbf{P})\,\hat{\mathbf{x}}_\mathrm{p}\,\mathrm{e}^{\mathrm{i}\,\Omega\,t}\right\}\ , \qquad (12)$$

where Ω represents angular frequency of kinematic excitation, generally different from shaft angular frequency ω. Stability properties given by solution of eigenvalue characteristics therefore do not depend on any kind of kinematic excitation $\mathbf{x}_\mathrm{p}$. On the other hand, the course of rotor response as an envelope of time-response amplitude vectors can be substantially changed and modelled by an appropriate choice of bushing trajectory parameters.

Provided that no bearing trajectory is prescribed, but external periodic forces act on bearing bushings, the entire system is described by two differential equations for shaft and bushings motion, with unbalance and bearing bushing forces on the right hand side of the equations. But this is still a linear system of differential equations, whose stability can depend neither on unbalance forces $\mathbf{n}(\omega,t)$ nor on kinematic exciting forces $\mathbf{f}_\mathrm{b}(\Omega,t)$.

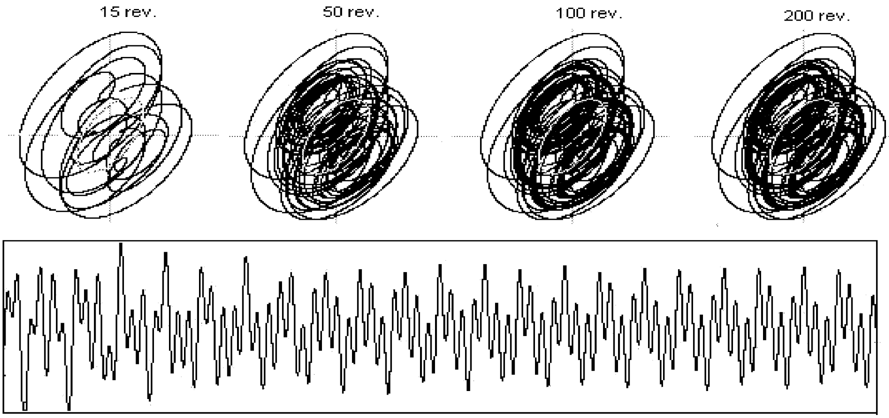

Fig.8: Stable orbit at 7000 rpm

To illustrate above-mentioned facts, concerning behaviour of the rotor under kinematic excitation of bearing bushings, simulation program for simple system of Laval's rotor was developed. Program enables to take harmonic bushing kinematic excitation either directly, in the form of elliptical bushing trajectory with non-synchronous frequency and optional forward/backward precession of motion, or indirectly by introducing external harmonic force acting on bearing bushings, naturally with similar parameters of excitation. The motion of the rotor is calculated by numerical integration of motion equations, which are described above.

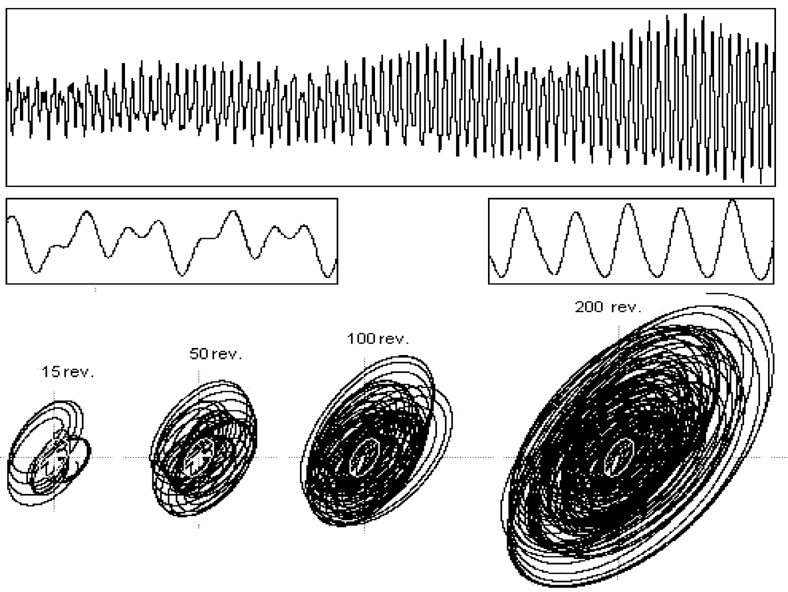

Fig.9: Unstable orbit at 8100 rpm

For numerical verification of the system stability two calculations for the same rotor-bearing configuration can be made alternatively: the 1st one with linearized bearing forces defined by a sequence of stiffness and damping matrices of the oil film, the 2nd one with general non-linear description of the field of hydrodynamic forces of a short journal bearing.

Parameters of this short bearing were chosen so that they best respond to the dynamic characteristics of test stand bearings.

An example of stable shaft trajectory in the non-linear field of hydrodynamic bearing forces at 7000 rpm is shown in figure 8. Bearing bushings were kinematically excited by harmonic backward rotating force with frequency 2000 rpm. Superposition of unbalance response with non-synchronous response of this kinematic bushing excitation is well visible n vibration time history diagram in vertical direction. The linearized calculation of the system predicts stability threshold at approximately 8200 rpm. However, as is shown in figure 9, the instability in case of non-linear system occurs a little sooner – at 8100 rpm, where self-excited vibrations with frequency $\approx$ 4100 rpm develop.

The situation described above was characteristic for all calculated examples of kinematic excitation of bearing bushings. In all cases, regardless of chosen excitation frequency, type of precession, direction and amplitude, self-excited vibration of the shaft occurred always at speeds near the predicted linear stability threshold. Usually, as in example demonstrated above, the non-linear stability threshold was a little lower than the predicted linear one.

6. Conclusion

The lumped parameter model of the journal centreline motion in the journal bearing is based on Muszynska's model and on Reynolds equation. The Muszynska's equation of motion contains the complex vector and parameters. The main goal of the simulation study was to verify the model principle by comparing simulation results with results of experiments. Test stand for investigation of journal bearing active control on rotor behaviour was designed and manufactured. Theoretical study was carried out in order to predict the effect of excitation mode on the rotor behaviour. It was shown, that kinematic excitation can affect amplitudes of vibration, but cannot influence stability limit. For suppression of rotor instability it will be apparently necessary to use more complicated excitation modes.

Acknowledgement

This research has been supported by the Czech Scientific Foundation as a part of the research project No. 101/07/1345.

References

[1] Muszynska A.: Whirl and Whip – Rotor/Bearing Stability Problems, Journal of Sound and Vibration (1986) 110(3), pp. 443–462
[2] Šimek, J.: Test stand for active control of sliding bearings with the aim to suppress rotor instability, Technical report No. 07-405, TECHLAB Ltd., 2007 (in Czech)
[3] Svoboda, R.: Theoretical analysis of influence of bearing bushing external excitation on dynamic properties of the rotor, Technical report No. 07-301, TECHLAB Ltd., 2007 (in Czech)
[4] Tůma J., Biloš J.: Fluid induced instability of rotor systems with journal bearings, Engineering Mechanics, Vol. 14, 2007, No. 1/2, p. 69–80, ISSN 1802-1484
[5] Muszynska A.: Rotordynamics, Taylor & Francis Group, New York 2005, ISBN 0-8247-2399-6
[6] Pinkus O., Sternlight B.: Theory of Hydrodynamic Lubrication, McGraw-Hill Book Company, New York 1961

Received in editor's office: March 25, 2008
Approved for publishing: July 29, 2008